**Climate
of the Past**

A high-resolution δ^{18}O record and Mediterranean climate variability

C. Taricco[1,2], G. Vivaldo[3], S. Alessio[1,2], S. Rubinetti[1], and S. Mancuso[2]

[1]Dipartimento di Fisica dell'Università di Torino, Turin, Italy
[2]Osservatorio Astrofisico di Torino (INAF), Pino Torinese, Italy
[3]IMT Institute for Advanced Studies, Lucca, Italy

Correspondence to: C. Taricco (carla.taricco@unito.it)

Abstract. A high-resolution, well-dated foraminiferal δ^{18}O record from a shallow-water core drilled from the Gallipoli Terrace in the Gulf of Taranto (Ionian Sea), previously measured over the last two millennia, has been extended to cover 707 BC–AD 1979. Spectral analysis of this series, performed using singular-spectrum analysis (SSA) and other classical and advanced methods, strengthens the results obtained analysing the shorter δ^{18}O profile, detecting the same highly significant oscillations of about 600, 380, 170, 130 and 11 years, respectively explaining about 12, 7, 5, 2 and 2 % of the time series total variance, plus a millennial trend (18 % of the variance). The comparison with the results of multi-channel singular-spectrum analysis (MSSA) applied to a data set of 26 Northern Hemisphere (NH) temperature-proxy records shows that NH temperature anomalies share with our local record a long-term trend and a bicentennial (170-year period) cycle. These two variability modes, previously identified as temperature-driven, are the most powerful modes in the NH temperature data set. Both the long-term trends and the bicentennial oscillations, when reconstructed locally and hemispherically, show coherent phases. Furthermore, the corresponding local and hemispheric amplitudes are comparable if changes in the precipitation–evaporation balance of the Ionian sea, presumably associated with temperature changes, are taken into account.

1 Introduction

The key to gaining information on climate analogues and periodicities, on decadal to multi-centennial and millennial timescales, is the measurement of proxy records over recent millennia, with multi-annual resolution and matching accuracy in dating.

Among the different timescales of natural climatic variability, the centennial scale is particularly interesting, being comparable to the scale of human life and to the modern variation related to anthropogenic forcing (Jones and Briffa, 1996; Jones et al., 1999, 2012).

The instrumental observations, covering only a couple of centuries (Ghil and Vautard, 1991; Martinson et al., 1995; Plaut et al., 1995; Jones et al., 1999, 2012, 2013; Folland and Karl, 2001; National Research Council of the National Academies, 1996), are influenced by human activity (Barnett et al., 1999) and are also too short to study centennial variability. In order to overcome this problem, several large-scale temperature reconstructions have been proposed, from both single-proxy (tree rings, corals, varved sediments, cave deposits, ice cores, boreholes, glaciers, and ocean and lake sediments) and multi-proxy records (Jones et al., 1998; Mann and Jones, 2003; Mann et al., 1999, 2008; Crowley, 2000; Moberg et al., 2005) deriving from different geographical locations: ice cores (Jones, 1996) for high latitudes, tree rings (Luckman et al., 1999; Esper et al., 2002) for mid-latitudes and corals (Crowley, 2000; Boiseau et al., 1999) for low latitudes. However, palaeoclimatic reconstructions depend on multiple, often uncontrolled, factors, e.g. multi-

proxy weighting and proxy calibration. These factors may lead to non-robust reconstructions (Lehner et al., 2012).

Marine cores with very high sedimentation rates allow for investigation of climate variations on scales of decades to millennia. In order to avoid possible artefacts produced by the composition of different proxies, we measured the oxygen isotopic ratio δ^{18}O in the shells of the surface-dwelling planktonic foraminifera *Globigerinoides ruber* in a high-resolution, well-dated central Mediterranean core. The isotopic composition of the shell, deposited on the sea bottom after the death of the organism, reflects the chemical and physical properties of marine surface waters, and therefore can give information about the environmental conditions in which the shell grew.

In a previous paper (Taricco et al., 2009) we presented a 2200-year-long foraminiferal δ^{18}O series and detected significant modes of variability from decadal to multicentennial scales, using singular-spectrum analysis (SSA) and other spectral methods. The isotopic profile showed features related to particular climatic periods, such as the low δ^{18}O values around AD 1000 (corresponding to the Medieval Warm Period – MWP), the high δ^{18}O values during the 18th century (corresponding to the Little Ice Age – LIA), the sudden decrease in δ^{18}O values starting from the 19th century (related to the temperature increase during the industrial era, and the high δ^{18}O values at the beginning of the Common Era, suggesting a local decrease in temperature.
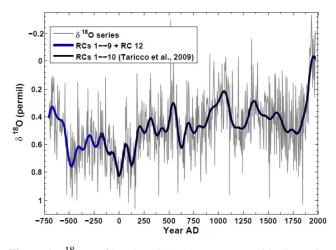
The record has now been extended to cover the last 2700 years. The aim of the present work is to investigate the spectral features of the prolonged series in order to detect the modes describing the climate variability over the interval 707–200 BC, in comparison with the following two millennia. Moreover, the results of a recent study by our group concerning Northern Hemisphere (NH) temperature and based on a reliable and extended data set (Taricco et al., 2014) allow for the local variability in the central Mediterranean to be compared with that characterizing NH.

2   Experimental procedure

Since the 1990s, the Torino cosmogeophysics group has been studying shallow-water Ionian Sea sediment cores, drilled from the Gallipoli Terrace in the Gulf of Taranto, and has carried out their absolute dating. The Gallipoli Terrace is a particularly favourable site for high-resolution climatic studies, due to a high sedimentation rate and to the possibility of accurate dating, offered by the presence along the cores of volcanic markers related to eruptive events that occurred in the Campanian area, a region for which documentation of the major eruptions is available. Historical documents are quite detailed for the last 350 years (a complete catalogue of eruptive events, starting from 1638, is given by Arnó et al., 1987), while they are rather sparse before that date.

The markers of the eruptions were identified along the cores as peaks of the number density of clinopyroxene crystals, carried by the prevailing westerly winds from the volcano to the Ionian Sea, and deposited there as part of marine sediments. The time–depth relation for the cores retrieved from the Gallipoli Terrace (Bonino et al., 1993; Cini Castagnoli et al., 1990, 1992, 1999, 2002a; Vivaldo et al., 2009) was obtained by tephroanalysis, which confirmed, improved and extended, to the deeper part of the core, the dating obtained in the upper 20 cm by the radiometric ^{210}Pb method (Krishnaswamy et al., 1971; Bonino et al., 1993). Taricco et al. (2008) further confirmed this dating by applying advanced statistical procedures (Guo et al., 1999; Naveau et al., 2003).

The cores were sampled every 2.5 mm, and the number density of clinopyroxenes of clear volcanic origin, characterized by skeletal morphology and sector zoning, was determined for the last two millennia. Twenty-two sharp pyroxene peaks, corresponding to historical eruptions of the Campanian area, starting from the Pompeii event in AD 79 and ending with the last Vesuvius eruption in AD 1944, were found. The depth h in centimetres at which a volcanic peak is found turned out to be related to the historical date of the corresponding eruption, expressed in years counted backward from AD 1979 (hence years before top, y_{BT}) by $h = (0.0645 \pm 0.0002) y_{BT}$, with a very high correlation coefficient ($r = 0.99$). The linearity of this relationship demonstrates that the sedimentation rate has remained constant over the last two millennia to a very good approximation. Moreover, the measurements performed in different cores retrieved from the same area showed that this rate is also uniform across the whole Gallipoli Terrace (Cini Castagnoli et al., 1990, 1992, 2002a, b). The very sharp pyroxene peaks indicate that bioturbation by bottom-dwelling organisms is quite limited; thus we were able to conclude that the climatic information obtained from these cores is not significantly affected by sediment mixing.

The series presented here was measured in the GT90/3 core (39°45′53″ N, 17°53′33″ E). In order to obtain the δ^{18}O value of each sample, we soaked 5 g of sediment in 5 % calgon solution overnight, then treated it in 10 % H_2O_2 to remove any residual organic material, and subsequently washed it with a distilled-water jet through a sieve with a 150 μm mesh. The fraction > 150 μm was kept and oven-dried at 50 °C. The planktonic foraminifera *Globigerinoides ruber* were picked out of the samples under the microscope. For each sample, 20 to 30 specimens were selected from the fraction comprised between 150 and 300 μm. The use of a relatively large number of specimens for each sample removes the isotopic variability of the individual organisms, giving a more representative δ^{18}O value. The stable isotope measurements were performed using a VGPRISM mass spectrometer fitted with an automated ISOCARB preparation device. Analytical precision based on internal standards is better than 0.1 ‰. Calibration of the mass spectrometer to

Figure 1. $\delta^{18}O$ profile (707 BC–AD 1979) measured in the Ionian GT90/3 core (grey line). In order to agree in tendency with temperatures, the isotopic ratio is plotted "upside down". The sampling interval is $\Delta t = 3.87\,y$, the raw data mean is $x_m = 0.47\,‰$ and their standard deviation is $\sigma = 0.23\,‰$. $\delta^{18}O$ signal reconstruction obtained by summing up its first 12 significant components extracted by SSA (blue line). The signal reconstruction obtained from the SSA analysis of the shorter, previously published $\delta^{18}O$ time series (Taricco et al., 2009) is shown as a black line. Except for a negligible border effect, the agreement between the two smooth curves is excellent over their common section ($r = 0.99$).

VPDB scale was done using NBS19 and NBS18 carbonate standards.

3 Results and discussion

In a previous paper (Taricco et al., 2009) we presented the $\delta^{18}O$ measurements performed in the upper 173 cm of the GT90/3 core (560 samples). The $\delta^{18}O$ series has now been extended, obtaining a continuous record of 694 points covering the last 2700 years (707 BC–AD 1979), shown in Fig. 1 (grey line). The high sampling rate ($\Delta t = 3.87$ years) makes this palaeoclimatic record suitable for the study of both long- and short-term variability components.

In Fig. 1, $\delta^{18}O$ is plotted "upside down" in order to agree in tendency with temperature. Since $\delta^{18}O$ reflects changes both in sea surface temperature (SST) and sea water isotopic composition, it is necessary to reliably extract independent components of variability and identify the temperature-driven ones.

Thus, several classical and advanced spectral methods were applied to the $\delta^{18}O$ time series, such as classical Fourier analysis, the maximum entropy method (MEM), singular-spectrum analysis (SSA) and the multi-taper method (MTM). Two review papers (Ghil and Taricco, 1997; Ghil et al., 2002) and references therein cover these methodologies. The application of more than one spectral method ensures that reliable information 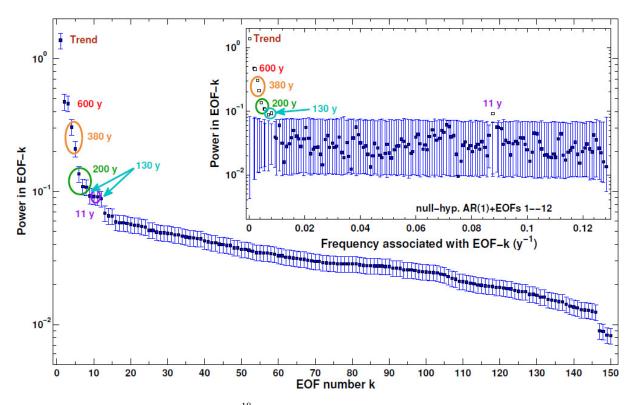is extracted from the $\delta^{18}O$ record, in spite of its low signal-to-noise ratio. Here we focus on the SSA results that were obtained using an embedding dimension $M = 150$, equivalent to a time window $M\Delta t \approx 600$ years, but we will also show that these results are stable to varying M over a wide range of values. We refer the interested reader to the Appendix for technical details on both SSA and Monte Carlo SSA (MC-SSA).

The SSA spectrum is shown in the main panel of Fig. 2, where the 150 eigenvalues are plotted in decreasing order of power.

At a first glance, we can notice a break between the initial steep slope (first 12 eigenvalues) and an almost flat floor. However, to reliably extract signal from noise, an MC-SSA test (MC-SSA; Allen and Robertson, 1996; Allen and Smith, 1996) was applied, showing that the first 12 eigenvalues are statistically significant at the 99 % confidence level (c.l.) and explain about 46 % of the $\delta^{18}O$ total variance.

The inset in Fig. 2 shows the results of the MC-SSA test. The error bars bracket 99 % of the eigenvalues obtained by the SSA of 5000 surrogate series, all of them generated by a null-hypothesis model that superposes empirical orthogonal functions (EOFs) 1–12 onto a red-noise process, i.e. an auto-regressive process of order 1, or AR(1). We can notice that only the eigenvalues associated with EOFs 1–12, the ones included in the null hypothesis and represented by empty squares, lie outside the 99 % error bars. This confirms that the model AR(1) + EOFs 1–12 captures the $\delta^{18}O$ variability at the 99 % c.l.; we drew this conclusion after rejecting, at the same confidence level, several null hypotheses, including different combinations of EOFs. Moreover, we chose red noise to accommodate the usual background assumption in geophysical applications, where the intrinsic inertia of the system leads to greater power at lower frequencies.

The significant components are a trend (EOF 1) explaining 17.7 % of total variance, and five oscillatory components of about 600 (EOFs 2–3), 380 (EOFs 4–5), 170 (EOFs 6–8), 130 (EOFs 9-12) and 11 years (EOFs 10–11), respectively explaining 12.0, 6.7, 4.6, 2.3 and 2.4 % of the total variance. The periods associated to each oscillation were evaluated by MEM. Figure 3 displays the reconstructions (Ghil and Vautard, 1991; Ghil and Taricco, 1997; Ghil et al., 2002) of the trend and the individual significant oscillations. In the same figure, these components (coloured lines) are compared with those obtained by the SSA of the shorter ($N = 560$) $\delta^{18}O$ time series, represented by black lines (Taricco et al., 2009). The agreement between the old and new reconstructed components is good; moreover, the small differences balance out if we consider the total reconstruction (RCs 1–12) of both the shorter and extended $\delta^{18}O$ time series (Fig. 1, black and blue smooth curves, respectively): the match between the two total reconstructions is excellent over their common time span, with a correlation coefficient $r = 0.99$. Only around the first century BC does the shorter series show a small border effect.

Figure 2. Eigenvalue spectrum from the SSA of the δ^{18}O record (window length $M = 150$). Each eigenvalue describes the fraction of total variance in the direction specified by the corresponding eigenvector (empirical orthogonal function – EOF). Inset: Monte Carlo SSA test using EOFs 1–12+AR(1) as the null-hypothesis model. The Monte Carlo ensemble size is 5000. The empty squares highlight the eigenvalues corresponding to the EOFs included in the null hypothesis, while the blue squares represent the eigenvalues corresponding to the remaining EOFs. No excursions occur outside the 99 % limits, indicating that the series is well explained by this model.

Thus, the SSA analysis of the longer δ^{18}O time series strengthens the results presented in our previous paper (Taricco et al., 2009), both detecting the same significant oscillations and, as a consequence, leading to the same signal reconstruction. In order to test the robustness of these results, we repeated the analysis, letting M vary over a wide range of values (100–250). Figure 4 shows the reconstructions of the 600-, 380- and 11-year oscillations for three values of M (150, 200 and 230). We notice that there is good agreement between the reconstructions corresponding to different values of M, so that the robustness of our analysis with respect to changes of the window is ensured.

The long-term variability features characterizing the δ^{18}O time series are captured by the trend (upper panel of Fig. 3), showing the pronounced maximum near AD 0, the minimum during the MWP (AD 900–1100) and the increase from the MWP toward the LIA. The 170-year oscillation, shown in the same figure, exhibits relative maxima around AD 1500, 1700 and 1900, possibly associated with the Spörer (AD 1460–1550), Maunder (AD 1645–1715) and modern minima of solar activity.
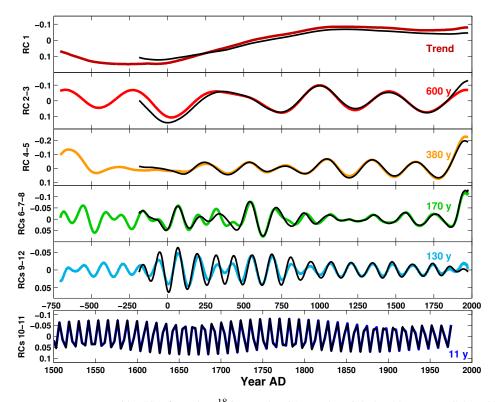
In order to compare the variability detected in the δ^{18}O profile with that characterizing Northern Hemisphere (NH) temperature, we constructed and analysed a data set of

26 temperature-proxy records, extending back at least to AD 1000 and having decadal or better resolution (Taricco et al., 2014). In order to ensure careful temperature calibration of the proxy data (Tingley et al., 2012), our data set contains only series satisfying the requirement that the temperature calibration of each proxy record be provided by the authors who published the record itself. The properties of the 26 records are listed in Table 1.

This data set was analysed using multi-channel singular-spectrum analysis (MSSA; see Keppenne and Ghil, 1993; Plaut and Vautard, 1994), a multivariate extension of SSA, with each *channel* corresponding to one of the time series of interest.

Application of SSA requires uniformly spaced time series; therefore, all the time series were interpolated to a common annual resolution. We then applied MSSA over the largest-possible common interval, spanning AD 1000 to 1935 (936 years; $N = 936$). We used a window length of 300 years, i.e. $M = 300 \leq N/3$.

High variance was found in the NH data set at both multi-decadal and centennial timescales, relative to what would be expected under the red-noise hypothesis. The significant reconstructed components are RCs 1–2 (trend), 6–

Figure 3. Significant components extracted by SSA from the δ^{18}O record: RC1 (trend), RC 2–3 (600 years), RC 4–5 (380 years), RCs 6–8 (170 years), RCs 9-12 (130 years) and RCs 10–11 (11 years). The black curves represent the reconstructions of the same oscillations provided by the analysis of the shorter, previously published δ^{18}O time series (Taricco et al., 2009).
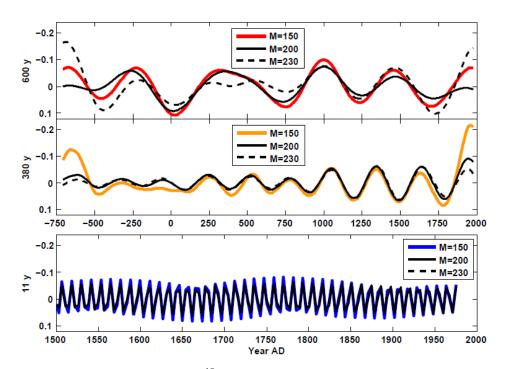

Figure 4. Reconstructed components from the SSA of the δ^{18}O time series, obtained adopting different values for the window length M.

8 (170 years), 9–10 (110 years), 12–13 (80 years), 16–17 (45 years) and 18–19 (60 years) (Taricco et al., 2014).

In our previous paper (Taricco et al., 2009), thanks to an alkenone-derived SST time series measured in cores extracted from the Gallipoli Terrace (Versteegh et al., 2007), we suggested that the long-term trend and the 200-year oscillation in the δ^{18}O record are temperature-driven. Here we notice that these two components dominate the spectrum of the NH temperature data set, which not only confirms that they are temperature-related but also that they characterize the dominant variability of the whole NH. These two modes also give the most important contributions to the net modern NH temperature rise (Taricco et al., 2014).
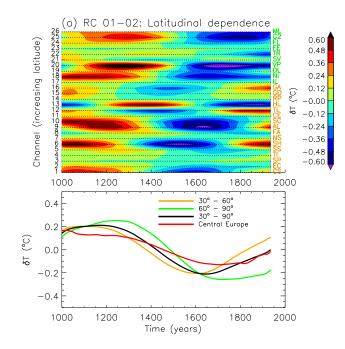
A centennial-scale periodicity is also in common between our local proxy record and NH temperature anomalies. However, spectral analysis of the 700-year-long local alkenone-based temperature record does not detect a centennial component (figure not shown) and therefore we can deduce that this climatic variability mode is not present locally. Its presence in the δ^{18}O record should thus derive from changes in the isotopic composition of sea water.

Focusing on the two dominant modes of NH temperature, in Figs. 5 and 6 we show their time behaviour reconstructed at each site, plotted in the upper panels of the figures in order of increasing latitude. In the lower panels we show the corresponding RC pairs averaged over two different latitude bands (30–60 and 60–90° N), as well as over the whole NH.

The trend (RCs 1–2) marks the MWP and the LIA climatic features and is present in both latitude belts. The cooler temperatures associated with the LIA appear first in mid-latitudes and propagate on to higher latitudes. The bicentennial oscillation (RCs 6–8; 170-year period), when averaged over the two different latitude belts, exhibits comparable amplitudes and a good phase agreement, as shown especially by the lower panel of Fig. 6.

Figure 7a compares the δ^{18}O and NH temperature trends. The two oscillations are in fair phase agreement: they exhibit nearly contemporary MWP features, while the LIA temperature minimum (δ^{18}O maximum) seems to have occurred slightly later at Gallipoli in respect to the whole NH. The average NH temperature decrease between the MWP and the LIA is of about 0.4 °C (black curve; also visible in the lower panel of Fig. 5). At mid-latitudes (30–60° N; orange curve in the lower panel of Fig. 5), the MWP–LIA temperature difference appears to be of the same order.

The individual series of the NH data set show, however, a certain difference in trend amplitudes (see the upper panel of Fig. 5). If we focus on the central Europe record (Büntgen et al., 2011), which is representative of a relatively large European area extending latitudinally from the Alps to northern Germany, we find a MWP–LIA decrease of the order of 0.3 °C. The alkenone-derived SST measurements from the Gallipoli Terrace (Versteegh et al., 2007), covering AD 1306–1979, show a local temperature decrease from ∼ 1300 to ∼ AD 1700 of about 0.5 °C, in agreement with NH

Figure 5. Reconstructed components RCs 1–2 of the NH temperature data set, representing the long-term trend; colour bar is for amplitude from −0.60 to 0.60 °C. Upper panel: RC pair of temperature anomalies from MSSA analysis as a function of increasing latitude; lower panel: the same RC pair averaged over two latitude bands, namely 30–60° N (orange) and 60–90° N (green), as well as over the entire NH (black). The red curve represents the trend of the central Europe series.
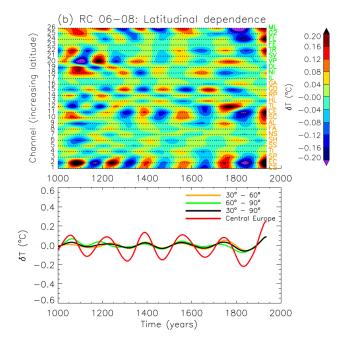
temperature, as may be expected for a long-term, global variation.

On the other hand, the MWP–LIA increase in the trend component of δ^{18}O (Fig. 7a, dark-red curve) is about 0.025 ‰: according to the Shackleton equation (Shackleton and Kennet, 1975), assuming a nearly constant oxygen isotopic ratio of sea water during the considered time interval, this variation would correspond to a cooling of ∼ 0.1 °C only. Thus at the Ionian Sea scale, δ^{18}O indicates a MWP–LIA temperature difference that is smaller than that found locally in the alkenone series, as well as hemispherically in the NH data set. This could be due to a contemporary change in the hydrological balance of the Ionian basin: a decrease in evaporation, accompanying the temperature decrease, would imply a reduction of the δ^{18}O of sea water and therefore a salinity increase (Pierre, 1999). Therefore the Ionian temperature MWP–LIA decrease, calculated from the Shackleton equation, would be greater than the one calculated assuming the δ^{18}O of sea water to be constant.

Using the alkenone-based MWP–LIA temperature variation of 0.5 °C, from the Shackleton equation we find that the +0.025 ‰ variation observed in the calcite δ^{18}O of foraminifera shells would be justified if the δ^{18}O of Ionian Sea water had varied, over the same time interval, by

Table 1. Characteristics of the 26 temperature time series in the NH data set. The columns in the table give a two-letter acronym; a full name based on the location; longitude; latitude; the archive from which the series was extracted; the proxy type; the time span; the sampling interval, Δt; and the published reference. The identification of the archives uses the following abbreviations: LS, lake sediments; IC, ice core; TR, tree rings; MS, marine sediments; MP, multi-proxy composite; ST, speleothems; DO, documentary.

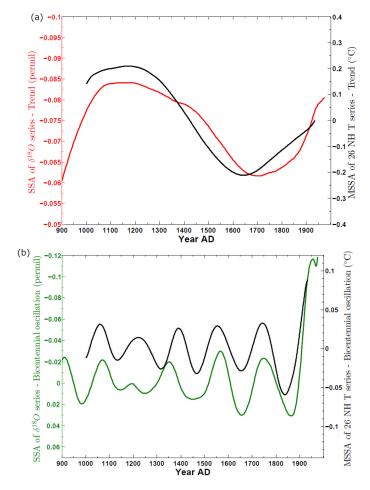| Acronym	Name	Long.	Lat.	Archive	Proxy type	Time span (yr)	Δt (yr)	Reference
ML	Lower Murray Lake	−69.32	81.21	LS	Mass accumul. rate	3236 BC–AD 1969	1	Cook et al. (2009)
G2	GISP2	−38.5	72.6	IC	δ^{15}N and δ^{40}Ar	2000 BC–AD 1993	1	Kobashi et al. (2011)
FL	Finnish Lapland	25	69	TR	Ring width	2000 BC–AD 2005	1	Helama et al. (2010)
FE	Fennoscandia (Laanila)	27.3	68.5	TR	Height increment	AD 745–2007	1	Lindholm et al. (2011)
TR	Torneträsk	19.80	68.31	TR	Density	AD 500–2004	1	Grudd (2008)
SV	Northern Scandinavia	25	68	TR	Density	138 BC–AD 2006	1	Esper et al. (2012)
VP	Vøring Plateau	7.64	66.97	MS	Foraminifer	883 BC–AD 1995	Irregular	Andersson et al. (2010)
DL	Donard Lake	−61.35	66.66	LS	Varve thickness	AD 752–1992	1	Moore et al. (2001)
NI	North Icelandic Shelf (MD99-2275)	−19.3	66.3	MS	$U^{37'}_K$ alkenone	2549 BC–AD 1997	Irregular	Sicre et al. (2011)
IL	Iceberg Lake	−142.95	60.78	LS	Varve thickness	AD 442–1998	1	Loso (2009)
GA	Gulf of Alaska	−145	60	TR	Ring width	AD 724–2002	1	Wilson et al. (2007)
GD	Gardar Drift (RAPiD21-3K)	−27.91	57.45	MS	$U^{37'}_K$ alkenone	5 BC–AD 1959	Irregular	Sicre et al. (2011)
RP	Russian Plains	45	45	MP	–	AD 5–1995	10	Sleptsov and Klimenko (2003)
HL	Hallet Lake	−146.2	61.5	LS	Biogenic silica	AD 116–2000	Irregular	McKay et al. (2008)
TL	Teletskoye Lake	87.61	51.76	LS	Biogenic silica	1018 BC–AD 2002	1	Kalugin et al. (2009)
CE	Central Europe (Alpine arc)	8	46	TR	Ring width	499 BC–AD 2003	1	Büntgen et al. (2011)
SC	Spannagel Cave	11.40	47.05	ST	δ^{18}O	90 BC–AD 1932	Irregular	Mangini et al. (2005)
AL	The Alps (Lötschental)	8.0	46.3	TR	Density	499 BC–AD 2003	1	Büntgen et al. (2006)
FA	French Alps	9	46	TR	Ring width	AD 751–2008	1	Corona et al. (2011)
NS	Northern Spain	−3.5	42.9	ST	δ^{13}C	1949 BC–AD 1998	Irregular	Martín-Chivelet et al. (2011)
SH	Shihua Cave	115.56	39.47	ST	Layer thickness	665 BC–AD 1985	1	Tan et al. (2003)
SS	Southern Sierra Nevada	−118.9	36.9	TR	Ring width	AD 800–1988	1	Graumlich (1993)
TI	Tibet	98.5	36.5	TR	Ring width	AD 1000–2000	1	Liu et al. (2009)
SP	Southern Colorado Plateau	−111.4	35.2	TR	Ring width	250 BC–AD 1996	1	Salzer and Kipfmueller (2005)
EC	East China	114	35	DO	Historical	AD 15–1977	Irregular	Ge et al. (2003)
CS	China Stack	100	35	MP	–	AD 0–1990	10	Yang et al. (2002)

Figure 6. Reconstructed components RCs 6–8 of the NH temperature data set, representing a bicentennial oscillation; colour bar for amplitude from −0.20 to 0.20 °C. Upper panel: RC pair of temperature anomalies from MSSA analysis as a function of increasing latitude; lower panel: the same RC pair averaged over two latitude bands, namely 30–60° N (orange) and 60–90° N (green), as well as over the entire NH (black). The red curve represents the bicentennial oscillation of the central Europe series.

Figure 7. Comparison between the reconstructed components extracted by SSA from the δ^{18}O profile and the corresponding oscillations extracted by MSSA from the NH temperature data set. **(a)** Long-term trend: δ^{18}O RC 1 (dark-red line) and NH temperature RCs 1–2 (black line); **(b)** 170-years oscillation: δ^{18}O RCs 6–8 (green line) and NH temperature RCs 6–8 (black line).

−0.1‰. This change would correspond, according to Pierre (1999), to a salinity decrease of about 0.4 PSU, a value that is of the order of the salinity variability range measured at Gallipoli during the last 60 years (Rixen et al., 2005).

We can thus state that the trend component of δ^{18}O reflects the long-term variations of NH temperature, provided that plausible changes in the hydrological balance of the Ionian basin are taken into account.

Turning now to the bicentennial component, we compare the δ^{18}O and NH temperature 170-year oscillations in Fig. 7b (green and black curves, respectively). The average amplitude for NH temperature is about 0.06 °C, but, as shown by the upper panel of Fig. 5, the amplitude of this component varies considerably from record to record in the NH data set. Among the individual local records we actually notice larger amplitudes, as in the case of central Europe, for which the 170-year oscillation amplitude is as large as 0.2 °C. This is not surprising, considering the shorter timescale considered here. The δ^{18}O amplitude is of the order of 0.4–0.5 ‰, which according to the Shackleton equation and in the absence of salinity variations would correspond to 0.2 °C, in agreement with central Europe. On the other hand, the Ionian alkenone-derived SST record has a bicentennial variation amplitude of about 1 °C (Taricco et al., 2009), which would imply a local

amplification effect in respect to European variability at this scale. This suggests that, also at this scale, it may be necessary to invoke salinity variations to explain the observed δ^{18}O variations.

4   Conclusions

A 2700-year-long, high-resolution record of foraminiferal δ^{18}O (Fig. 1) measured in a sediment core drilled in the Gulf of Taranto (Ionian Sea) was analysed using advanced spectral methods. Singular-spectrum analysis (SSA) of the series (Fig. 2) allowed for detection of the presence of a long-term trend and of highly significant oscillatory components with periods of roughly 600, 380, 170, 130 and 11 years, thus confirming the results found by Taricco et al. (2009), who analysed the previously published time series covering 188 BC–AD 1979 (Figs. 1, 3, and 4).

The construction of a data set of 26 temperature-proxy records, extending back at least to AD 1000 with at least decadal resolution and selected requiring that the temperature calibration of each proxy record be provided by the authors who published the record itself, allowed for the variability detected in the δ^{18}O profile to be compared with that present in reliable Northern Hemisphere (NH) temperature series published by other authors. The analysis of this data set, performed using multi-channel singular-spectrum analysis (MSSA), showed as dominant modes a millennial trend and an oscillation of $\sim$ 170 years (Figs. 5 and 6). Thus NH temperature anomalies share with our local record a long-term variation and a bicentennial cycle. The comparison of the corresponding reconstructed oscillations (Fig. 7) proved that these two components, previously identified as temperature-driven (Taricco et al., 2009) and representing the most powerful variability modes in the NH temperature data set, have coherent local and hemispheric phases. Moreover, the corresponding amplitudes are comparable if we allow for changes in the precipitation–evaporation balance of the Ionian Sea presumably associated with temperature changes.

Appendix A

A1 Singular-spectrum analysis (SSA)

Singular-spectrum analysis (SSA) is a non-parametric spectral estimation method which was originally designed to obtain information about non-linear systems from short and noisy time series without appealing to the process governing equations (Vautard and Ghil, 1989; Ghil and Vautard, 1991; Vautard et al., 1992; Ghil and Taricco, 1997; Ghil et al., 2002). SSA provides insight into the unknown or partially known dynamics of the underlying dynamical system by allowing the identification of different components of the analysed signal, such as trends, oscillatory patterns and random noise, without requiring any a priori model.

SSA grounds on the Mañé–Takens delay embedding theorem, according to which the dynamics of a chaotic dynamical system can be reconstructed from a single time series by its time-delayed embedding (Mañé, 1981; Takens, 1981). The so-obtained extended phase space is defined by a new orthogonal basis, which describes most of the variance in the original time series by a minimal number of components. Broomhead and King (1986) proposed the application of principal component analysis (PCA) in order to find the optimal solution to that optimization problem.

In contrast to a classical Fourier decomposition, the new orthogonal basis is data-adaptive and not restricted to pure sine and cosine functions. Thus, SSA turns out to be a more flexible and less limited spectral analysis method, especially when dealing with highly noisy, volatile, and often nonstationary experimental time series.

In more detail, given a time series $\{x(t), t = 1, \ldots, N\}$ of length N, an M-dimensional phase space is built by using M lagged copies of x:

$$X = \begin{pmatrix} x(1) & x(2) & \ldots & x(M) \\ x(2) & x(3) & \ldots & x(M+1) \\ \vdots & \vdots & \ldots & \vdots \\ x(N-M+1) & x(N-M+2) & \ldots & x(N) \end{pmatrix}. \quad \text{(A1)}$$

Selecting the window length M involves a trade-off between, on the one hand, the amount of spectral information, such as the number of peaks, one may gain on the time series and, on the other hand, the degree of signal-to-noise enhancement and the associated statistical confidence. The choice of M (see also Vautard et al., 1992; Ghil et al., 2002) thus corresponds to a compromise between including more peaks for larger M – while taking into account that periods longer than M cannot be resolved – and achieving a higher degree of statistical significance for the peaks detected, at smaller M. In general, the stable features of the eigenset – i.e. of the set of eigenvalues and eigenvectors – can be evaluated by varying the window size M over a given range, $M_1 \leq M \leq M_2$.

From the augmented time series X, the covariance matrix is computed as $C = X^T X / N$.

The Toeplitz approach by Vautard and Ghil (1989) is applied in order to ensure the stability of entries c_{ij} along (sub-and super-)diagonals of covariance matrix. That way,

$$c_{ij} = \frac{1}{N - |i - j|} \sum_{t=1}^{N - |i - j|} x(t) x(t + |i - j|) \quad \text{(A2)}$$

are constants which depend only on the lag $|i - j|$.

Next, the symmetric covariance matrix is diagonalized,

$$\Lambda = E^T C E, \quad \text{(A3)}$$

to yield a diagonal matrix Λ of eigenvalues λ_k and an orthogonal matrix E of eigenvectors. The columns e_k of E represent the new M-dimensional coordinate system and λ_k describes the variance of X in the direction of e_k. The variance of the original time series $x(t)$ is preserved in the eigenvalues, which now lie along the main diagonal of Λ.

By projecting the time series $x(t)$ onto each of the M eigenvectors e_k, M principal components (PCs) are obtained:

$$a_k(t) = \sum_{j=1}^{M} x(t + j - 1) e_k(j), \quad \text{(A4)}$$

with $1 \leq t \leq N - M + 1$.

Although PCs exhibit no exact phase information, it is possible to analyse various aspects of the time series that belong to the direction e_k by computing its reconstructed component (RC),

$$r_k(t) = \frac{1}{M_t} \sum_{j=L_t}^{U_t} a_k(t - j + 1) e_k(j), \quad \text{(A5)}$$

where $(M_t, L_t, U_t) = (M, 1, M)$ for $M \leq t \leq N - M + 1$; for either end interval refer to Ghil et al. (2002).

No information is lost during the reconstruction process, since the superposition of all individual RCs, $x(t) = \sum_{k=1}^{M} r_k(t)$, gives the original time series (Vautard et al., 1992).

A2 Monte Carlo SSA

A critical step when performing spectral analysis is the distinction of significant oscillations from random fluctuations. Allen and Smith (1996) have proposed a stringent test, relying on a sophisticated null hypothesis, which takes the possibility of spurious oscillations into account. Based on a Monte Carlo simulation technique, the extracted spectral components are tested against a red-noise hypothesis, i.e. an autoregressive process of order 1, AR(1),

$$X(t) = a_1 [X(t-1) - X_0] + \sigma \xi(t) + X_0; \quad \text{(A6)}$$

here X_0 is the process mean and ξ a normally distributed white-noise process with zero mean and unit variance.

That way, Monte Carlo SSA (MC-SSA) can be used to establish whether a given time series is linearly distinguishable

from any well-defined process, including the output of a deterministic chaotic system.

The coefficients a_1 and σ are estimated from the time series using a maximum-likelihood criterion. An ensemble of surrogate time series is then generated from the AR(1) process and compared with the real data. In practice, the covariance matrix $\boldsymbol{C}_R$ is firstly estimated for each AR(1) realization and then projected onto the eigenvectors $\boldsymbol{E}$ of the original data:

$$\boldsymbol{\Lambda}_R = \boldsymbol{E}^{\mathrm{T}} \boldsymbol{C}_R \boldsymbol{E}. \tag{A7}$$

The projection allows one to determine the degree of resemblance between the surrogates generated by the test and the original data by computing statistics on the diagonal elements. From the ensemble distribution of λ_R along the diagonal, we are able to obtain significance intervals outside which the time series' eigenvalues can be considered to be significantly different from an AR(1) process in Eq. (A6). Note that a rejection of the most likely AR(1) process leads to a rejection of all other red-noise processes, at the same or at an even higher level of significance (Ghil et al., 2002).

References

Allen, M. R. and Robertson, A. W.: Distinguishing modulated oscillations from coloured noise in multivariate datasets, Clim. Dynam., 12, 775–784, 1996.

Allen, M. R. and Smith, L. A.: Monte Carlo SSA: detecting irregular oscillations in the presence of colored noise, J. Climate, 9, 3373–3404, 1996.

Andersson, C., Pausata, F. S. R., Jansen, E., Risebrobakken, B., and Telford, R. J.: Holocene trends in the foraminifer record from the Norwegian Sea and the North Atlantic Ocean, Clim. Past, 6, 179–193, doi:10.5194/cp-6-179-2010, 2010.

Arnó, V., Principe, C., Rosi, M., Santacroce, R., Sbrana, A., and Sheridan, M. F.: Eruptive history, in: Summa-Vesuvius, Quaderni de La Ricerca Scientifica, edited by Santacroce R., CNR, Roma, Italy, 114, 53–103, 1987.

Barnett, T. P., Hasselmann, K., Chelliah, M., Delworth, T., Hegerl, G., Jones, P. D., Rasmusson, E., Roeckner, E., Ropelewski, C., Santer, B., and Tett, S.: Detection and attribution of recent climate change: a status report, B. Am. Meteorol. Soc., 80, 2631–2659, 1999.

Boiseau, M., Ghil, M., and Juillet-Leclerc, A.: Climatic trends and interdecadal variability from South-Central Pacific coral records, Geophys. Res. Lett., 26, 2881–2884, 1999.

Bonino, G., Cini Castagnoli, G., Callegari, E., and Zhu, G. M.: Radiometric and tephroanalysis dating of recent Ionian sea cores, Nuovo Cimento C, 16, 155–161, 1993.

Broomhead, D. S. and King, G.: Extracting qualitative dynamics from experimental data, Physica D, 20, 217–236, 1986.

Büntgen U., Frank, D. C., Nievergelt, D., and Esper, J.: Summer temperature variations in the European Alps, AD 755–2004, J. Climate, 19, 5606–5623, 2006.

Büntgen, U., Tegel, W., Nicolussi, K., McCormick, M., Frank, D., Trouet, V., Kaplan, J. O., Herzig, F., Heussner, K. U., Wanner, H., Luterbacher, J., and Esper, J.: 2500 years of European climate variability and human susceptibility, Science, 331, 578–582, 2011.

Cini Castagnoli, G., Bonino, G., Caprioglio, F., Provenzale, A., Serio, M., and Zhu, G. M.: The carbonate profile of two recent Ionian sea cores: evidence that the sedimentation rate is constant over the last millenia, Geophys. Res. Lett., 17, 1937–1940, 1990.

Cini Castagnoli, G., Bonino, G., Provenzale, A., Serio, M., and Callegari, E.: The CaCO$_3$ profiles of deep and shallow Mediterranean sea cores as indicators of past solar-terrestrial relationship, Nuovo Cimento C, 15, 547–563, 1992.

Cini Castagnoli, G., Bonino, G., Della Monica, P., Taricco, C., and Bernasconi, S. M.: Solar activity in the last millennium recorded in the δ^{18}O profile of planktonic foraminifera of a shallow water Ionian Sea core, Solar Phys., 188, 191–202, 1999.

Cini Castagnoli, G., Bonino, G., and Taricco, C.: Long term solar-terrestrial records from sediments: Carbon isotopes in planktonic foraminifera during the last millennium, Adv. Space Res., 29, 1537–1549, 2002a.

Cini Castagnoli, G., Bonino, G., Taricco, C., and Bernasconi, S. M.: Solar radiation variability in the last 1400 years recorded in the carbon isotope ratio of a Mediterranean sea core, Adv. Space Res., 29, 1987–1994, 2002b.

Cook, T. L., Bradley, R. S., Stoner, J. S., and Francus, P.: Five thousand years of sediment transfer in a High Arctic watershed recorded in annually laminated sediments from Lower Murray Lake, Ellesmere Island, Nunavut, Canada, J. Paleolimnol., 41, 77–94, 2009.

Corona, C., Edouard, J. L., Guibal, F., Guiot, J., Bernard, S., Thomas, A., and Denelle, N.: Long-term summer (AD 751–2008) temperature fluctuation in the French Alps based on tree-ring data, Boreas, 40, 351–366, 2011.

Crowley, T. J.: Causes of climate change over the past 1000 years, Science, 289, 270–277, doi:10.1126/science.289.5477.270, 2000.

Esper, J., Cook, E. R., and Schweingruber, F. H.: Low-frequency signals in long tree-ring chronologies for reconstructing past temperature variability, Science, 295, 2250–2253, doi:10.1126/science.1066208, 2002.

Esper J., Frank, D. C., Timonen, M., Zorita, E., Wilson, R. J. S., Luterbacher, J., Holzkämper, S., Fischer, N., Wagner, S., Nievergelt, D., Verstege, A., and Büntgen, U.: Orbital forcing of tree-ring data, Nat. Clim. Chang., 2, 862–866, 2012.

Folland, C. K. and Karl, T. R.: Recent rates of warming in marine environment meet controversy, Eos, Trans. AGU, 82, 453–461, doi:10.1029/01EO00270, 2001.

Ge, Q., Zheng, J., Fang, X., Man, Z., Zhang, X., Zhang, P., and Wang, W. C.: Winter half-year temperature reconstruction for the middle and lower reaches of the Yellow River and Yangtze River, China, during the past 2000 years, Holocene, 13, 933–940, 2003.

Ghil, M. and Taricco, C.: Advanced spectral analysis methods, in: Past and Present Variability of the Solar-terrestrial System: Measurement, Data Analysis and Theoretical Models, edited by: Cini Castagnoli, G. and Provenzale, A., IOS Press, Amsterdam, the Netherlands, 137–159, 1997.

Ghil, M. and Vautard, R.: Interdecadal oscillations and the warming trend in global temperature time series, Nature, 350, 324–327, 1991.

Ghil, M., Allen, M. R., Dettinger, M. D., Ide, K., Kondrashov, D., Mann, M. E., Robertson, A. W., Saunders, A., Tian, Y., Varadi, F., and Yiou, P.: Advanced spectral methods for climatic time series, Rev. Geophys., 40, 3.1–3.41, doi:10.1029/2000RG000092, 2002.

Graumlich, L. J.: A 1000-yr record of temperature and precipitation in the Sierra Nevada, Quaternary Res., 39, 249–255, 1993.

Grudd, H.: Torneträsk tree-ring width and density AD 500–2004: a test of climatic sensitivity and a new 1500-year reconstruction of North Fennoscandian summers, Clim. Dyn., 31, 843–857, 2008.

Guo, W., Wang, Y., and Brown, M. B.: A signal extraction approach to modelling hormone time series with pulses and a changing baseline, J. Am. Stat. Assoc., 94, 746–756, 1999.

Helama, S., Macias Fauria, M., Mielikäinen, K., Timonen, M., and Eronen, M.: Sub-Milankovitch solar forcing of past climates:

mid and late Holocene perspectives, Geol. Soc. Am. Bull., 122, 1981–1988, 2010.

Jones, P. D.: Climate variations and forcing mechanisms of the last 2000 Years, edited by: Bradley, S., and Jouzel, J., NATOASI Series I, Springer-Verlag, Berlin, Germany, 649 pp., 1996.

Jones, P. D. and Briffa, K. R.: What can the instrumental record tell us about longer timescale paleoclimatic reconstructions, in: Climatic Variations and Forcing Mechanisms of the Last 2000 Years, Springer-Verlag, Berlin, 625–644, 1996.

Jones, P. D., Briffa, K. R., Barnett, T. P., and Tett, S. F. B.: High-resolution palaeoclimatic records for the last millennium: interpretation, integration and comparison with General Circulation Model control-run temperatures, Holocene, 8, 455–471, 1998.

Jones, P. D., New, M., Parker, D. E., Martin, S., and Rigor, I. G.: Surface air temperature and its changes over the past 150 years, Rev. Geophys., 37, 173–199, 1999.

Jones, P. D., Lister, D. H., Osborn, T. J., Harpham, C., Salmon, M., and Morice, C. P.: Hemispheric and large-scale land-surface air temperature variations: An extensive revision and an update to 2010, J. Geophys. Res., 117, D05127, doi:10.1029/2011JD017139, 2012.

Jones, P. D., Parker, D. E., Osborn, T. J., and Briffa, K. R.: Global and hemispheric temperature anomalies – land and marine instrumental records, in Trends: A Compendium of Data on Global Change, Carbon Dioxide Information Analysis Center, Oak Ridge National Laboratory, US Department of Energy, Oak Ridge, Tenn., USA, doi:10.3334/CDIAC/cli.002, 2013.

Kalugin, I. A., Daryin, A. V., and Babich, V. V.: Reconstruction of annual air temperatures for three thousand years in Altai region by lithological and geochemical indicators in Teletskoe Lake sediments, Dokl. Earth Sci., 426, 681–684, 2009.

Keppenne, C. L. and Ghil, M.: Adaptive filtering and prediction of noisy multivariate signals: An application to subannual variability in atmospheric angular momentum, Intl. J. Bifurcation Chaos, 3, 625–634, 1993.

Kobashi, T., Kawamura, K, Severinghaus, J. P., Barnola, J.-M., Nakaegawa, T., Vinther, B. M., Johnsen, S. J., and Box, J. E.: High variability of Greenland surface temperature over the past 4000 years estimated from trapped air in an ice core, Geophys. Res. Lett., 38, L21501, doi:10.1029/2011GL049444, 2011.

Krishnaswamy, S., Lal, D., Martin, J. M., and Meybeck, M.: Geochronology of lake sediments, Earth Planet. Sc. Lett., 11, 407–414, 1971.

Lehner, F., Raible, C. C., and Stocker, T. F.: Testing the robustness of a precipitation proxy-based North Atlantic Oscillation reconstruction, Quaternary Sci. Rev., 45, 85–94, doi:10.1016/j.quascirev.2012.04.025, 2012.

Lindholm, M., Jalkanen, R., Salminen, H., Aalto, T., and Ogurtsov, M.: The height-increment record of summer temperature extended over the last millennium in Fennoscandia, Holocene, 21, 319–326, 2011.

Liu, Y., An, Z. S., Linderholm, H. W., Chen, D. L., Song, H. M., Cai, Q. F., Sun, J. Y., and Tian, H.: Annual temperatures during the last 2485 years in the mid-eastern Tibetan Plateau inferred from tree rings, Sci. China Ser. D, 52, 348–359, 2009.

Loso, M. G.: Summer temperatures during the Medieval Warm Period and Little Ice Age inferred from varved proglacial lake sediments in Southern Alaska, J. Paleolimnol., 41, 117–128, 2009.

Luckman, B. H., Briffa, K. R., Jones, P. D., and Schweingruber, F. H.: Tree-ring based reconstruction of summer temperatures at the Columbia Icefield, Alberta, Canada, AD 1073–1983, Holocene, 7, 375–389, 1999.

Mañé, R.: On the dimension of the compact invariant sets of certain non-linear maps. In: Dynamical Systems and Turbulence, Vol. 898 of Lecture Notes in Mathematics, Springer, Berlin, 230–242, 1981.

Mangini, A., Spötl, C., and Verdes, P.: Reconstruction of temperature in the Central Alps during the past 2000 yr from a δ^{18}O stalagmite record, Earth Planet. Sc. Lett., 235, 741–751, 2005.

Mann, M. E. and Jones, P. D.: Global surface temperatures over the past two millennia, Geophys. Res. Lett., 30, 1820–1823, doi:10.1029/2003GL017814, 2003.

Mann, M. E., Bradley, R. S., and Hughes, M. K.: Northern Hemisphere temperatures during the past millennium: Inferences, uncertainties, and limitations, Geophys. Res. Lett., 26, 759–762, 1999.

Mann, M. E., Zhang, Z., Hughes, M. K., Bradley, R. S., Miller, S. K., and Rutherford, S.: Proxy-based reconstructions of hemispheric and global surface temperature variations over the past two millennia, P. Natl. Acad. Sci., 105, 13252–13257, doi:10.1073/pnas.0805721105, 2008.

Martín-Chivelet, J., Muñoz-García, M. B., Edwards, R. L., Turrero, M. J., and Ortega, A. I.: Land surface temperature changes in Northern Iberia since 4000 yr BP, based on δ^{13}C of speleothems, Global Planet. Change, 77, 1–12, 2011.

Martinson, D. G., Bryan, K., Ghil, M., Hall, M. M., Karl, T. R., Sarachik, E. S., Sorooshian, S., and Talley, L. D. (Eds.): Natural climate variability on decade-to-century time scales, in: National Research Council of the National Academies, National Academy Press, Washington DC, USA, 630 pp., 1995.

McKay, N. P., Kaufman, D. S., and Michelutti, N.: Biogenic silica concentration as a high-resolution, quantitative temperature proxy at Hallet Lake, South-central Alaska, Geophys. Res. Lett., 35, L05709, doi:10.1029/2007GL032876, 2008.

Moberg, A., Sonechkin D. M., Holmgren, K., Datsenko, N. M., and Karlén, W.: Highly variable Northern Hemisphere temperatures reconstructed from low- and high-resolution proxy data, Nature, 433, 613–617, 2005.

Moore, J. J., Hughen, K. A., Miller, G. H., and Overpeck, J. T.: Little Ice Age recorded in summer temperature reconstruction from varved sediments of Donard Lake, Baffin Island, Canada, J. Paleolimnol., 25, 503–517, 2001.

National Research Council of the National Academies: Surface temperature reconstructions for the last 2000 years, National Academy Press, Washington DC, USA, 145 pp., 2006.

Naveau, P., Ammann, C., Oh, H. S., and Guo, W.: An automatic statistical methodology to extract pulse-like forcing factors in climatic time series: Application to volcanic events, edited by: Robock, A., Volcanism and the Earth's Atmosphere, Geophysical Monograph, 139, 177–186, 2003.

Pierre, C.: The oxygen and carbon isotope distribution in the Mediterranean water masses, Mar. Geol., 153, 41–55, 1999.

Plaut, G. and Vautard, R.: Spells of low-frequency oscillations and weather regimes in the Northern Hemisphere, J. Atmos. Sci., 51, 210–236, 1994.

Plaut, G., Ghil, M., and Vautard, R.: Interannual and interdecadal variability in 335 yr of Central England temperatures, Science, 268, 710–713, 1995.

Rixen, M., Beckers, J.-M., Levitus, S., Antonov, J., Boyer, T., Maillard, C., Fichaut, M., Balopoulos, E., Iona, S., Dooley, H., Garcia, M.-J., Manca, B., Giorgetti, A., Manzella, G., Mikhailov, N., Pinardi, N., Zavatarelli, M., and the Medar Consortium: The Western Mediterranean Deep Water: a proxy for climate change, Geophys. Res. Lett., 32, L12608, doi:10.1029/2005GL022702, 2005.

Salzer, M. W. and Kipfmueller, K. F.: Reconstructed temperature and precipitation on a millennial timescale from tree-rings in the Southern Colorado Plateau, USA, Climatic Change, 70, 465–487, 2005.

Shackleton, N. J. and Kennett, J. P.: Palaeo-temperature history of the Cenozoic and the initiation of Antarctic glaciation: Oxygen and carbon isotope analysis in DSDP sites 277, 279 and 281, in: Initial Reports of the Deep Sea Drilling Project, edited by: Kennet, J. P. and Houtz, R. E., US Government Printing Office, Washington, DC, USA, 5, 743–755, 1975.

Sicre M.-A., Hall, I. R., Mignot J., Khodri, M., Ezat, U., Truong, M.-X., Eiríksson, J., and Knudsen, K.-L.: Sea surface temperature variability in the subpolar Atlantic over the last two millennia, Paleoceanography, 26, PA4218, doi:10.1029/2011PA002169, 2011.

Sleptsov, A. M. and Klimenko, V. V.: Multi-proxy reconstruction of the climate of Eastern Europe during the last 2000 yr, Izvestya of the Russian Geographical Society, 6, 45–54, 2003 (in Russian).

Takens, F.: Detecting strange attractors in turbulence. In: Dynamical Systems and Turbulence, Vol. 898 of Lecture Notes in Mathematics, Springer, Berlin, 366–381, 1981.

Tan, M., Liu T. S., Hou, J., Qin, X., Zhang, H., and Li, T.: Cyclic rapid warming on centennial-scale revealed by a 2650-year stalagmite record of warm season temperature, Geophys. Res. Lett., 30, 1617–1620, doi:10.1029/2003GL017352, 2003.

Taricco, C., Alessio, S., and Vivaldo, G.: Sequence of eruptive events in the Vesuvio area recorded in shallow-water Ionian Sea sediments, Nonlin. Processes Geophys., 15, 25–32, doi:10.5194/npg-15-25-2008, 2008.

Taricco, C., Ghil, M., Alessio, S., and Vivaldo, G.: Two millennia of climate variability in the Central Mediterranean, Clim. Past, 5, 171–181, doi:10.5194/cp-5-171-2009, 2009.

Taricco, C., Mancuso, S., Ljungqvist, F. C., Alessio, S., and Ghil, M.: Multispectral analysis of Northern Hemisphere temperature records over the last five millennia, Clim. Dynam., doi:10.1007/s00382-014-2331-1, 2014.

Tingley, M. P., Craigmile, P. F., Haran, M., Li, B., Mannshardt, E., and Rajaratnam, B.: Piecing together the past: statistical insights into paleoclimatic reconstructions, Quaternary Sci. Rev., 35, 1–22, 2012.

Vautard, R. and Ghil, M.: Singular spectrum analysis in nonlinear dynamics, with applications to paleoclimatic time series, Physica D, 35, 395–424, 1989.

Vautard, R., Yiou, P., and Ghil, M.: Singular spectrum analysis: a toolkit for short noisy chaotic signals, Physica D, 58, 95–126, 1992.

Versteegh, G. J. M., de Leeuw, J. W., Taricco, C., and Romero, A.: Temperature and productivity influences on $U_K^{37'}$ and their possible relation to solar forcing of the Mediterranean winter, Geochem. Geophy. Geosy., 8, Q09005, doi:10.1029/2006GC001543, 2007.

Vivaldo, G., Taricco, C., Alessio, S., and Ghil, M: Accurate dating of Gallipoli Terrace (Ionian Sea) sediments: Historical eruptions and climate records, PAGES News, 17, 8–9, 2009.

Wilson, R., Wiles, G., D'Arrigo, R., and Zweck, C.: Cycles and shifts: 1,300 years of multi-decadal temperature variability in the Gulf of Alaska, Clim. Dynam., 28, 425–440, 2007.

Yang, B., Braeuning, A., Johnson, K. R., and Yafeng, S.: Temperature variability in the subpolar Atlantic over the last two millennia, Geophys. Res. Lett., 29, 38-1–38-4, doi:10.1029/2001GL014485, 2002.